JEE Journal of Ecological Engineering

Journal of Ecological Engineering, 2026, 27(11), 392–403
https://doi.org/10.12911/22998993/231147
ISSN 2299–8993, License CC-BY 4.0

Received: 2026.07.13
Accepted: 2026.09.15
Published: 2026.10.01

Fungal-mediated valorization of rice bran and eggshell waste into calcite-rich bio-composites: Characterization and potential for cementitious applications

Maria Mathayo Mdende[1,2*], Yusufu Abeid Chande Jande[1], Nelson Mpumi[1], Shadrack Sabai[2]

[1] Nelson Mandela African Institute of Science and Technology, P.O. Box 447, Arusha, Tanzania
[2] Ardhi University, P.O. Box 35176, Dar Es Salaam, Tanzania
* Corresponding author's e-mail: mdendem@nm-aist.ac.tz

ABSTRACT

This study investigated the potential of agro-waste-derived substrates to support fungal-mediated biomineralization of calcium carbonate for the production of calcite-rich biocomposites with potential cementitious applications. Rice bran powder and eggshell powder were evaluated as organic nutrient and calcium sources, respectively, to support the growth of *Penicillium* sp. isolated from environmental soil samples. Five experimental treatments were monitored over a 28-day incubation period and characterized using XRD, XRF, and FTIR. The integrated system (T5) exhibited an initial decrease in pH to 5.89, followed by pH recovery to 8.14 by Day 28, indicating changes in the chemical environment during incubation that were favorable for calcium carbonate precipitation. T5 exhibited a 21.53% reduction in solid-phase mass during incubation. Quantitative Rietveld analysis indicated that calcite accounted for 100% of the quantified crystalline phase assemblage in T5, with no detectable aragonite or vaterite within the resolution and detection limits of the analysis. The Rietveld refinement yielded an Rwp of 9.14%, indicating reasonable agreement between the experimental and calculated diffraction profiles. XRF analysis showed a high CaO content (46.04%) together with silica and potassium in the resulting material. FTIR spectroscopy identified organic functional groups and carbonate-associated vibrational bands, providing complementary evidence for the organic and inorganic components of the product. These findings indicated that rice bran and eggshell wastes can serve as alternative organic nutrient and calcium sources, respectively, for *Penicillium* sp. to produce calcite-rich material for sustainable cementitious applications.

Keywords: *Penicillium* sp., calcium carbonate precipitation, eggshell powder, fungal biomineralization, calcite formation.

INTRODUCTION

Concrete cracking is a pervasive structural issue triggered by mechanical loading, environmental stressors, and the use of low-quality materials in buildings (Singh and Bhandari, 2024; Taoufik et al., 2024). These cracks compromise building stability and have led to catastrophic collapses globally, resulting in significant loss of life, injuries, and property damage buildings globally (Adetunji et al., 2018; Kioko, 2014; Ohenhen and Shirzaei, 2022; Singh and Bhandari, 2024; Taoufik et al., 2024). For instance, structural defects and soil settling have caused persistent cracking in major infrastructure in Tanzania, endangering public safety (Magafu and Li, 2010). Despite various maintenance efforts, the occurrence of cracks remains a critical challenge that threatens the long-term integrity and resilience of the built environment (Jaf and Abdulrahman, 2023; Udhaya et al., 2023).

Conventional methods for repairing concrete cracks typically rely on cementitious binders or polymer resins, such as epoxies, to seal open surfaces (Jaf and Abdulrahman, 2023; Udhaya et al., 2023). However, cementitious-based materials often suffer from high shrinkage, poor corrosion resistance, potential toxicity, and limited compatibility with the existing cement matrix, leaving structures vulnerable to early-age cracking and long-term degradation (Zhao et al., 2025). Also, polymer materials such as epoxy resin have been widely used to seal cracks due to their adhesive properties to concrete, but it's potential toxicity, susceptibility to aging, and poor compatibility with cementitious-based materials have been shown as their limitations (Zhao et al., 2025). While Microbial-Induced Calcite Precipitation (MICP) using bacteria has emerged as a promising alternative, it faces significant practical hurdles (Zhang et al., 2024). Bacteria such as *Bacillus pasteurii*, *Bacillus sphaericus,* and *Bacillus cohnii* are used as biological methods for crack healing, which is effective for crack widths of up to 0.5 mm, and leads to $CaCO_3$ precipitation due to the strong bond between cement and aggregate (Saxena et al., 2024). However, the bacterial method has several limitations, including low survivability in concrete due to limited nutrients. Some studies have supplemented bacteria with nutrients such as urea, calcium chloride, and yeast extract, yet these chemical supplements cause corrosion and long-term durability concerns caused by chloride ion reactions (Omoregie et al., 2024).There are limited studies which applied other types of microbes like fungi. Therefore, this study aimed to investigate the fungal-mediated conversion of rice bran and eggshell waste into a calcite-rich biocomposite for potential application in self-healing cementitious materials. Specifically, the study presents the effect of rice bran content on the physicochemical characteristics of the fungal-mediated biocomposites, monitored changes in pH over 28 days, and characterized the resulting mineralogical and chemical properties using X-ray diffraction (XRD), Fourier-transform infrared spectroscopy (FTIR), and X-ray fluorescence (XRF).

MATERIALS AND METHODS

Isolation of *Penicillium* sp. and substrate preparation

The fungal strain used in this study was isolated from soil samples collected at the Maji ya Chai dump site and the Nelson Mandela African Institution of Science and Technology (NM-AIST) banana farm. A serial dilution (10^{-1} to 10^{-5}) was performed in 90 mL of sterile distilled water, and 1 mL of each dilution was plated onto potato dextrose agar (PDA) augmented with 50 mg/L chloramphenicol to inhibit bacterial growth. Following incubation at 25–28 °C for 5–7 days, colonies exhibiting the velvety texture and green color with white margins characteristic of *Penicillium* sp. were selected and purified through 2–3 rounds of sub-culturing. Identification of *Penicillium* sp. was confirmed microscopically by staining with lactophenol cotton blue to observe the branched, brush-like conidiophores and spherical conidia.

For the biomineralization substrates, chicken eggshells were collected from broiler chickens in Arusha, washed, oven-dried at 105 °C for 24 h, and sieved to 32 μm. Rice bran was obtained from local mills, oven-dried to remove moisture, ground, and then sieved to a particle size of 125 μm to ensure consistency.

Experimental design and incubation conditions

The experiment consisted of five treatments designed to evaluate the interactions between the *Penicillium* sp fungi and agro-waste substrates in 500 mL glass bottles containing 250 mL of sterile distilled water, as shown in Table 1. Treatment one (T1) served as the baseline (fungal spores + water), treatment two (T2) composed of rice bran, fungal spores and water (Rice bran powder + Fungal Spores + Sterile Water), treatment three (T3) composed of eggshells, fungal spores and water (Eggshell Powder + Fungal Spores + Sterile Water), treatment four composed of an abiotic control containing rice bran (5 g) and eggshells (1.25 g) without fungal inoculation (Table 1), and treatment five (T5) was an integrated system containing both the substrates and the fungal strain (Table 1). All mixtures were autoclaved at 121 °C for 15 min before adding two fungal agar plugs to the respective treatments. The systems were then incubated on a rotary shaker at 120 rpm at 28±2 °C for 28 days (Figure 1).

Analytical measurements and characterization

Biochemical changes were monitored by measuring the pH on days 0, 7, 14, and 28 using a Thermo Scientific Orion Versa Star Pro Benchtop pH Meter manufactured by Thermo Fisher Scientific in Waltham, Massachusetts, United States.

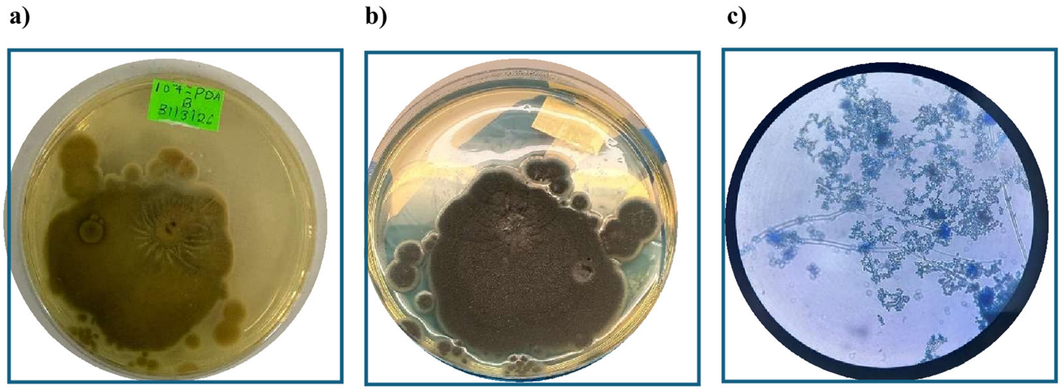

Figure 1. *Penicillium* sp. (a) reverse morphological appearance, (b) front morphological appearance, (c) microscopic appearance

On days 14 and 28, the biomass-mineral composite yield was recovered by an H2500R 6 × 100 mL High-Speed Refrigerated Centrifuge manufactured by Cence Centrifuge in Hunan, China, at 3000 rpm for 15 min. The resulting residues were treated with 10 mL of 70% ethanol to denature the fungal biomass and then dried in a Heratherm Large Capacity Oven manufactured by Thermo Scientific in Langenselbold, Germany, at 100 °C for 3 h prior to final weighing using an analytical balance manufactured by Precision Industry Scale in China. The structural evolution of the precipitates was analyzed using X-ray diffraction (XRD) and X-ray fluorescence (XRF) with an ARL 9800 Oasis X-Ray System, manufactured by Thermo ARL in Ecublens, Switzerland. Phase quantification (calcite, aragonite, and vaterite) was performed using Profex 5.7 software. Finally, molecular functional groups were identified through Fourier Transform Infrared Spectroscopy (FTIR) using a Nicolet 6700 spectrometer manufactured by Thermo Electron Corporation in Madison, Wisconsin, United States, where spectra were scaled using the Amide I peak (1630–1650 cm^{-1}) to standardize protein signatures across the samples.

Table 1. Mixing ratios

Treatment	Eggshell Powder (g)	Rice bran powder (g)	Fungal spore plugs (count)
T1	0	0	2
T2	0	5	2
T3	1.25	0	2
T4	1.25	5	0
T5	1.25	5	2

RESULTS AND DISCUSSION

pH variation

From Table 2, the pH evolution from Day 0 to Day 28 revealed distinct biochemical and mineral interactions across the treatment systems, driven by fungal metabolic activity, rice bran substrate degradation, and eggshell-derived calcium carbonate buffering. One-way analysis of variance (ANOVA) was used to determine whether treatment composition significantly influenced pH variation throughout the study. The F-statistic represents the ratio of the variability in pH among treatment means to the residual variability in pH within treatments, with larger F-values indicating greater variability in mean pH among treatments relative to within treatments. One-way analysis of variance (ANOVA) confirmed that the treatment composition significantly influenced pH variation throughout the study: Day 0 ($F = 4986.97$, $p < 0.001$), Day 7 ($F = 1345.22$, $p < 0.001$), Day 14 ($F = 688.59$, $p < 0.001$), and Day 28 ($F = 2095.16$, $p < 0.001$). At Day 0, initial differences were governed by the chemical nature of the inputs; whereby Treatment 3 (T3: eggshell + fungi) exhibited significantly ($F = 4986.97$, $P < 0.001$) higher (9.40 ± 0.02) pH indicating alkalinity when compared to all other treatments according to Tukey's HSD test, while the rice bran-containing treatments T4 and T5 were statistically similar with the pH values of 7.26 ± 0.06 and 7.31 ± 0.01, respectively. By Day 7, the results revealed significant acidification in fungal treatments containing rice bran, with T2 (rice bran + fungi) dropping to 5.19 ± 0.00 and T5 (rice bran + eggshell + fungi) to 5.88 ± 0.05. The acidification observed in treatments T2 and T5 indicates active fungal metabolism, where carbohydrates from rice bran were utilized to produce organic acids, a phase that is critical for the mobilization of Ca from mineral sources. These results concur with other researchers who reported that fungal metabolisms in carbohydrates found in rice bran lead to the formation of organic acids, and this lowered the pH of the bio-composite materials (Lee et al., 2016; Lelamurnik et al., 2017).

In contrast, systems dominated by eggshells, such as T3, maintained alkaline conditions throughout (7.90 to 8.27), reflecting the strong buffering effect of calcium carbonate (Le et al., 2026; Ohshima et al., 2015; Vasquez et al., 2024). By Day 14, a transition toward neutral-to-alkaline conditions was observed, with T4 (7.91 ± 0.01) and T5 (7.87 ± 0.02) showing no significant statistical difference, suggesting that fungal activity in the complete system (T5) successfully restored alkaline conditions suitable for mineral precipitation. This pH recovery in T5 favors biomineralization, where mobilized Ca^{2+} ions combine with carbonate ions at fungal hyphae nucleation sites to form crystals (Mony, 2015; Yan et al., 2024). By Day 28, the pH values further stabilized, indicating progression from the initial substrate degradation phase to the biomineral maturation stage. Treatment three (T3) remained the most alkaline treatment (8.34 ± 0.04) owing to the continuous buffering capacity of eggshell-derived calcium carbonate. However, T5 increased to 8.14 ± 0.04^{b}, demonstrating significant recovery from the acidic conditions observed on Day 7. This increase in pH suggests that after rice bran-driven fungal metabolism and calcium mobilization, the system shifted toward favourable conditions for $CaCO_3$ precipitation. The significantly higher pH of T5 compared to T2 (6.45 ± 0.03) further demonstrates that eggshell-derived calcium carbonate is essential for maintaining alkalinity and supporting fungal-induced mineral formation. This pH trend highlights a two-stage biomineralization mechanism: an early stage of rice bran-driven acidification for calcium release, followed by a later stage of eggshell-mediated buffering and pH recovery, which facilitates the formation of calcite. This biologically consolidated environment in T5 is distinct from simple physical mixtures, as confirmed by the statistical separation in ANOVA and Tukey's HSD analyses.

Solid-phase transformation during fungal biomineralization

The observed changes in Figure 2, precipitate mass over the 28-day incubation period, demostrate a significant interrelationship between fungal growth, substrate utilization, and calcium carbonate biomineralization. From Table 3, Treatment 5 (rice bran + eggshell + fungi) exhibited a high mass reduction of 21.53% (from 4.63 g to 3.63 g), which exceeded the abiotic loss observed in Treatment 4 (18.87%), suggesting that fungal activity significantly accelerated substrate transformation beyond natural leaching processes. In contrast, Treatment 2 (rice bran + fungi) showed a 23.71% reduction, indicating that rice bran serves as a vital carbon and nutrient reservoir that stimulates fungal biomass production and extracellular enzyme secretion (Ahmed et al., 2017; Denardi et al., 2019; Wainaina et al., 2020). The minimal mass loss in Treatment 3 (1.17%) further confirms that eggshells alone cannot adequately support fungal metabolism and organic acid production necessary for mineral transformation without a supplementary organic nutrient source (Li et al., 2018). While T5 showed a substantial reduction in total recovered mass, this signified the successful conversion of heterogeneous agro-wastes into a stabilized biomass-mineral composite rather than a lack of biomineral formation (Bindschedler et al., 2016; Denardi et al., 2019; Li et al., 2014; Li et al., 2018; Wainaina et al., 2020). In

Table 2. pH variation

Treatment	pH at day 0	pH at day 7	pH at day 14	pH at day 28
T1	8.84±0.01^{b}	6.55±0.24^{b}	6.55±0.07^{c}	6.58 ± 0.03^{d}
T2	6.17±0.01^{d}	5.19±0.00^{e}	6.14±0.01^{d}	6.45 ± 0.03^{e}
T3	9.40±0.02^{a}	7.90±0.03^{a}	8.27±0.03^{a}	8.34 ± 0.04^{a}
T4	7.26±0.06^{c}	6.17±0.01^{c}	7.91±0.01^{b}	7.98 ± 0.04^{c}
T5	7.31±0.01^{c}	5.89±0.05^{d}	7.87±0.02^{b}	8.14 ± 0.04^{b}
F-value	4986.97	1345.22	688.59	2095.16
p-value	< 0.001	< 0.001	< 0.001	< 0.001

Table 3. Weight of recovered biomass-mineral composite

Treatment	Weight at day 0 (g)	Weight at day 14 (g)	Weight at day 28 (g)
T1	0.02 ± 0.00^{e}	0.02 ± 0.00^{e}	0.05 ± 0.01^{e}
T2	3.67 ± 0.02^{c}	3.04 ± 0.02^{c}	2.80 ± 0.02^{c}
T3	1.11 ± 0.01^{d}	1.04 ± 0.01^{d}	1.09 ± 0.02^{d}
T4	4.17 ± 0.03^{b}	3.54 ± 0.03^{a}	3.38 ± 0.02^{b}
T5	4.63 ± 0.03^{a}	3.34 ± 0.03^{b}	3.63 ± 0.03^{a}
F-value	34429.206	18550.82459	17778.72951
p-value	< 0.001	< 0.001	< 0.001

this integrated system, fungal organic acids promote the partial dissolution of eggshell-derived calcium carbonate, facilitating the reorganization of calcium phases into stable carbonate minerals. By Day 28, a shift in the recovered biomass-mineral composite mass was observed, indicating progression from the initial substrate degradation phase toward mineral stabilization and biomineral accumulation. One-way ANOVA confirmed that significant differences ($F = 17778.73$, $p < 0.001$) among the treatments remained on day 28, demonstrating that substrate composition continued to influence composite formation. Unlike T2, which further decreased from 3.04 ± 0.017 g at Day 14 to 2.80 ± 0.020 g at Day 28 due to the continued degradation of rice bran organic fractions, T5 increased from 3.34 ± 0.030 g to 3.633 ± 0.031 g. This recovery suggests that after the initial fungal utilization of rice bran and calcium mobilization from eggshells, biomineral precipitation became the dominant process. The significantly higher Day 28 recovered mass of T5 compared with the other treatments, according to Tukey's HSD test ($p < 0.05$), confirms the synergistic contribution of fungal activity, organic nutrients, and calcium availability in promoting the formation of a stable biomass-$CaCO_3$ composite. Ultimately, the synergistic combination of rice bran-derived nutrients, eggshell-derived calcium, and fungal metabolic activity in T5 created the most favourable microenvironment for the development of calcite-rich bio-composites, indicating its potential as a precursor material for sustainable cementitious applications.

XRD of precipitation yield

XRD analysis of Day 28 residues observed in Figure 3 confirmed distinct structural differences across treatments. The diffraction pattern, as shown in Figure 3 of T5, exhibited a combination of a broad diffuse hump at 20–25° 2θ, attributed to amorphous fungal biomass, together with sharp reflections at 30°, 37°, 43°, 47°, and 48° 2θ, corresponding to crystalline calcite. These sharp reflections align with established calcite crystallography, where the strongest diffraction peak typically occurs between 29–30° 2θ (Priya and Kannan, 2025). T2 exhibited a broad diffuse hump centred approximately at 20–25° 2θ, with no clearly resolved reflections characteristic of crystalline calcium carbonate. This pattern indicates a predominantly amorphous structure, potentially associated with the organic/fungal biomass and other non-crystalline components of the precipitate. In contrast, T3, T4, and T5 exhibited distinct sharp diffraction reflections, particularly around 29–30°, 36–37°, 39–43°, and 47–49° 2θ, indicating the formation of crystalline calcium carbonate. The prominent reflection near 29–30° 2θ is characteristic of calcite and is consistent with previously reported calcite diffraction patterns (Mariyam et al., 2025; Priya and Kannan, 2025).

To further identify and quantify the crystalline calcium carbonate phases, Rietveld refinement was performed using Profex 5.7 with the BGMN refinement engine. The refinement models, as shown in Figure 4, included calcite, aragonite, and vaterite as candidate crystalline $CaCO_3$ polymorphs. Cu Kα radiation ($\lambda = 1.5410$ Å) was used, and the diffraction data were refined over the measured 2θ range. The refinement considered the experimental diffraction pattern, calculated pattern, background contribution, and phase-specific reflection positions. The fitted patterns, experimental profiles, difference curves, and calculated reflection markers for the refined samples are presented in Figure 4.

The refinement results demonstrated that calcite was the predominant crystalline phase in all three eggshell-containing treatments, as shown in Table 4. For T3, the refined phase composition

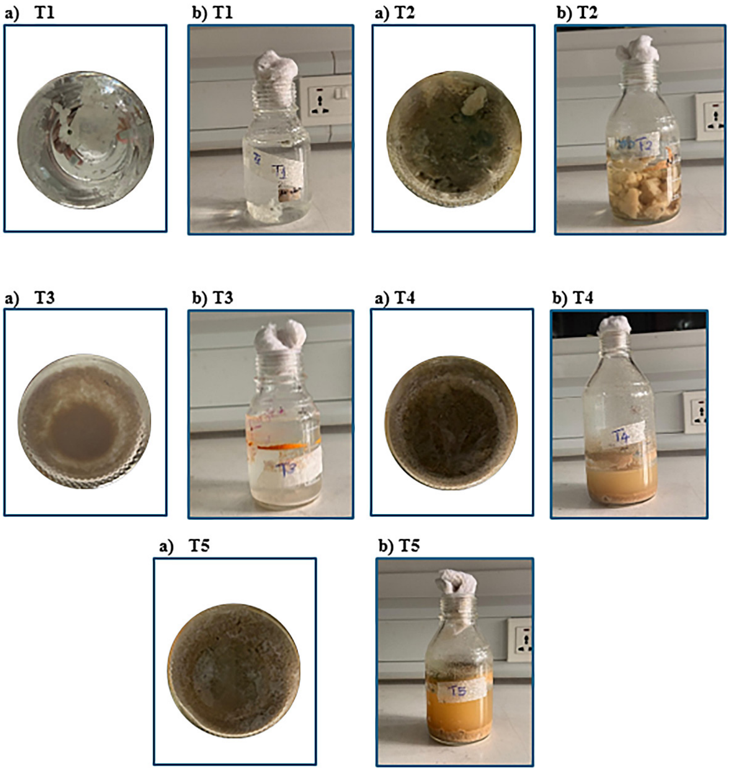

Figure 2. Biomass-mineral composites were observed in the following treatments: (T1) sterile water and fungal spores, (T2) rice bran and fungal spores, (T3) eggshell and fungal spores, (T4) rice bran and eggshell without fungal spores, and (T5) rice bran, eggshell, and fungal spores. Pictures taken from (a) the bottom of the glass bottle of the culture and (b) the side of the glass bottle of the culture

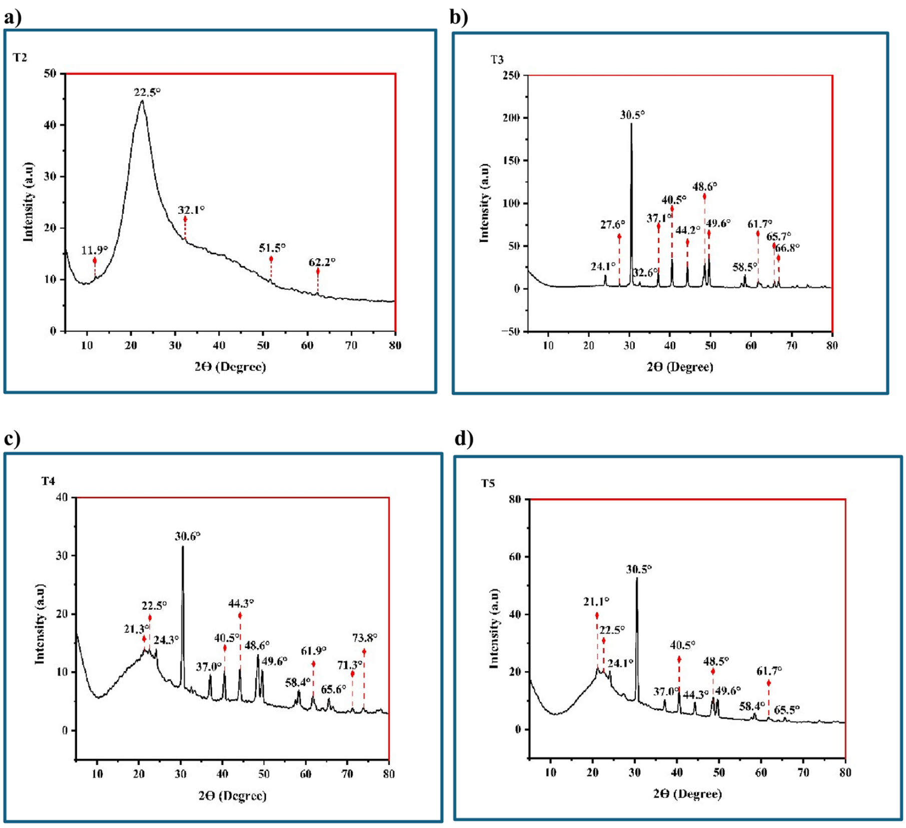

Figure 3. X-Ray Diffraction of biomass-mineral composite: (a) T2, (b) T3, (c) T4, and (d) T5

a)

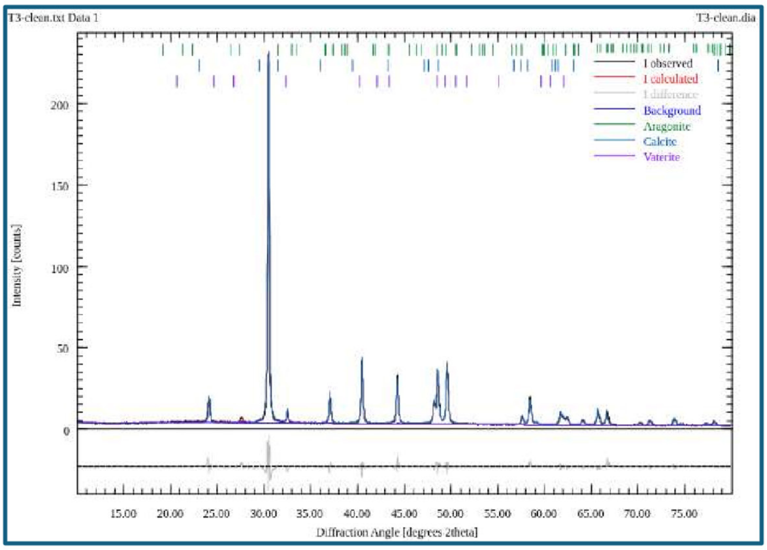

b)

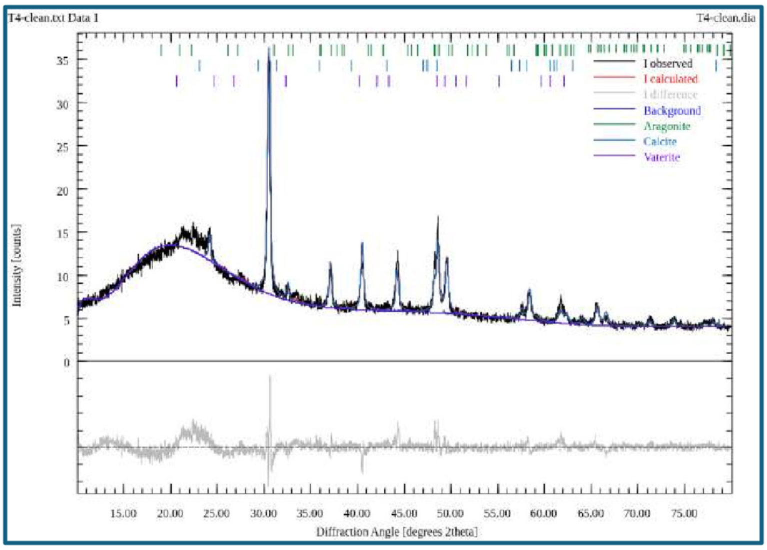

c)

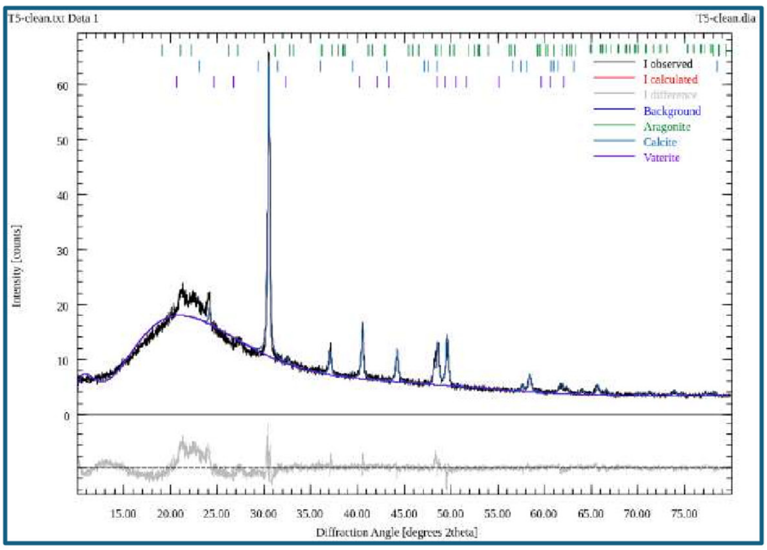

Figure 4. Rietveld refinement plots of the XRD patterns of (a) T3, (b) T4, and (c) T5, showing experimental and calculated profiles, background, difference curves, and phase-specific reflection

was 98.01 wt.% calcite, 0.83 wt.% aragonite, and 1.16 wt.% vaterite. T4 contained 97.23 wt.% calcite, 0.67 wt.% aragonite, and 2.10 wt.% vaterite. In T5, the refinement assigned 100.00 wt.% of the quantified crystalline phase to calcite, with aragonite and vaterite refined to 0 wt.%. These results indicate that calcite overwhelmingly dominated the crystalline $CaCO_3$ fraction, while the minor aragonite and vaterite contributions detected in T3 and T4 were comparatively small.

The goodness-of-fit statistics further indicated reasonable agreement between the calculated and experimental profiles. The refined Rwp values were 9.85%, 7.42%, and 9.14% for T3, T4, and T5, respectively, while the corresponding χ^2 values were 0.0520, 0.0409, and 0.0678. The fitted profiles and relatively low residual differences demonstrate that the selected crystalline-phase models provided a reasonable representation of the major diffraction features observed in the experimental patterns. Nevertheless, the quantitative phase proportions should be interpreted as the distribution of the detected crystalline phases within the refinement model, rather than as the total composition of the precipitates rather than the total composition of the residues, because this crystalline-phase refinement does not quantitatively represent amorphous material.

XRF of precipitation yield

Table 5 shows the XRF analysis on Day 28, which provided quantitative confirmation of elemental redistribution and successful biomineralization, with calcium oxide (CaO) being identified as the dominant phase across all mineral-containing treatments, that is, T2 to T5. Treatment 3 (T3) recorded the highest CaO content (52.52%), which is consistent with its primarily eggshell-based composition and aligns with established evidence that chicken eggshells are mainly composed of $CaCO_3$ (Spelta and Galdino, 2018). In the integrated system, T5 exhibited 46.04% CaO, a value closely comparable to the abiotic control T4 (46.59%), demonstrating that the biomineralization process effectively retains and concentrates calcium within the fungal-mineral matrix rather than losing it during biological transformation (Setiyawan et al., 2021; Sompech et al., 2016). Notably, Treatment 2 (T2) exhibited 35.01% CaO, indicating that rice bran inherently contributes measurable calcium that is incorporated into the fungal biomass during growth. Beyond calcium, secondary oxide fractions revealed the significant influence of rice bran-derived elements; silica (SiO_2) was highest in T2 (12.61%) and remained significant in T5 (5.57%), confirming its origin from agricultural residues

Table 4. Phase composition and refinement quality of the biomass-mineral composite

Treatment	Calcite (wt.%)	Vaterite (wt.%)	Aragonite (wt.%)	Rwp	Rexp	χ^2
T3	98.01	1.16	0.83	9.85	43.19	0.0520
T4	97.23	2.10	0.67	7.42	36.71	0.0409
T5	100	0	0	9.14	35.11	0.0678

Table 5. Elemental composition of the biomass-mineral composite samples

Elemental composition	T2 (%)	T3 (%)	T4 (%)	T5 (%)
CaO	35.01	52.52	46.59	46.04
MgO	1.71	0.30	1.27	1.40
K_2O	6.70	0.12	1.76	2.45
Na_2O	0.07	0.08	0.07	0.07
MnO	0.18	0.00	0.07	0.07
SO_3	0.78	0.04	0.33	0.05
P_2O_5	0.00	0.00	0.00	0.02
TiO_2	0.36	0.06	0.13	0.14
SiO_2	12.61	2.04	5.54	5.57
Al_2O_3	1.71	0.91	1.12	1.28
Fe_2O_3	5.88	0.67	0.57	0.72
LOI	34.73	42.85	42.07	41.21

(Sompech et al., 2016). Potassium oxide (K_2O) also showed elevated levels in T2 (6.70%) and enrichment in T5 (2.45%) relative to T4 (1.76%), suggesting fungal-mediated mineral accumulation during metabolic growth (Wikandari et al., 2025). These XRF results validate a coherent chemical transformation pathway, where T5 successfully integrates organic nutrient retention with inorganic mineral consolidation. This results in a stabilized, silica-supported, calcium-rich composite that demonstrates an effective route for converting agricultural wastes into calcium-rich functional biomaterials with potential engineering applications (Simpen et al., 2024).

Fourier transform infrared spectroscopy (FTIR)

Fourier transform infrared spectroscopy (FTIR) spectral analysis revealed changes in the functional-group profiles across the treatments, providing complementary information to the structural characteristics identified by XRD and the elemental composition determined by XRF. Treatment 2 (T2) was dominated by organic functional groups, where aliphatic C-H stretching bands at 2922 and 2852 cm^{-1} were associated with lipid-containing groups as observed by Smidt et al., (2002), and a strong C-O vibration at 1037 cm^{-1} was consistent with the presence of polysaccharide-rich biomass (Niemeyer et al., 1992). The detection of a carbonyl band at 1709 cm^{-1} in T2 was consistent with the presence of carbonyl-containing organic compounds, which may be associated with organic acids formed during fungal fermentation, a key metabolic process in rice bran degradation, as shown in Figure 5 for T2. In contrast, Figure 5 for T3 exhibited a spectrum dominated by calcium carbonate signatures, specifically the asymmetric stretching band at 1398 cm^{-1} and the bending bands at 873 and 712 cm^{-1}, which are characteristic of carbonate minerals and crystalline calcite, respectively (Cahya and Marfuah, 2014; Ningrum et al., 2022).

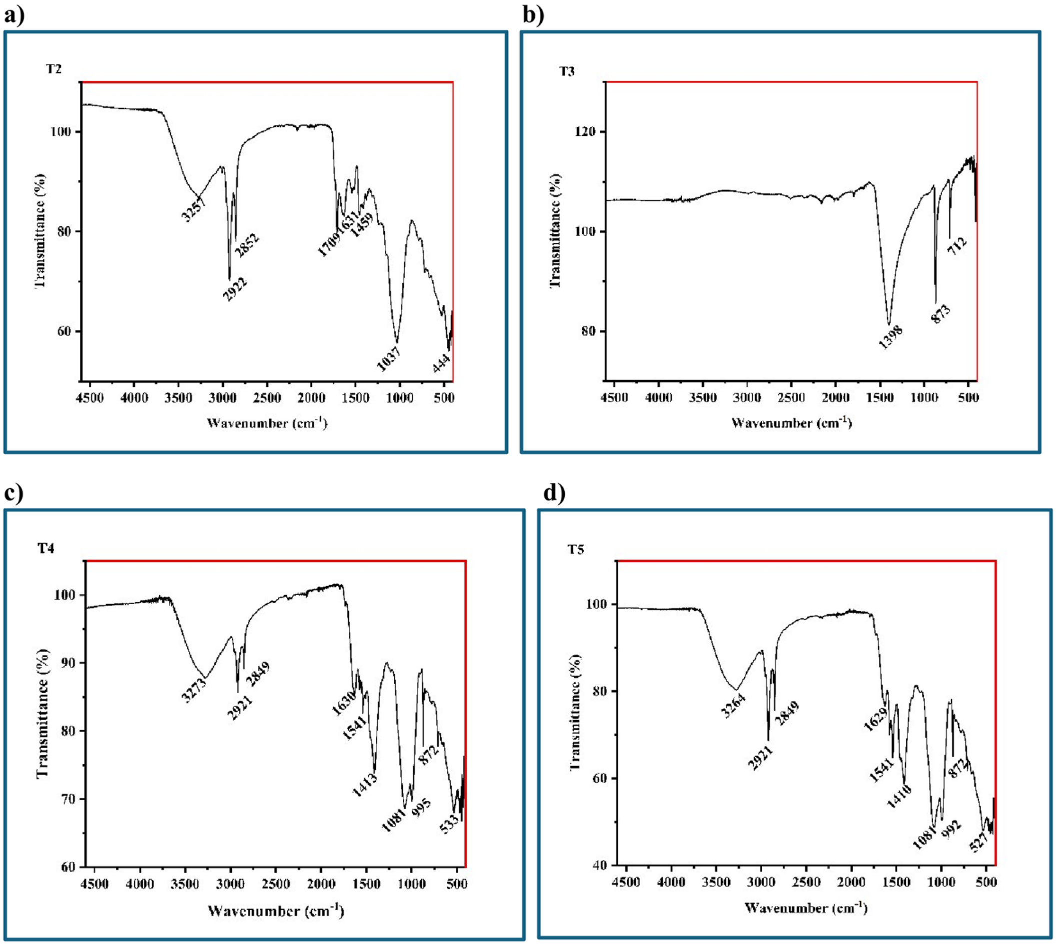

Figure 5. Fourier transform infrared spectroscopy of biomass-mineral composite: (a) T2, (b) T3, (c) T4, and (d) T5

In T5, the spectrum exhibited O-H/N-H stretching at 3264 cm^{-1} and Amide I and II bands at 1629 and 1541 cm^{-1}, respectively, which are associated with protein-containing organic matter (Lopes et al., 2018; Parikh and Chorover, 2005; Preston et al., 2011). Simultaneously, as shown in Figure 4 for T5, the appearance of pronounced carbonate-associated bands at 1410 and 872 cm^{-1} in T5 was consistent with the presence of $CaCO_3$ in the composite. The slight shift of the carbonate band from 1413 cm^{-1} in the abiotic control (T4) to 1410 cm^{-1} in T5 may indicate a change in the local chemical environment of the carbonate groups (Yusuf, 2023). This spectral difference suggested possible interactions between the organic and inorganic components of the composite, although FTIR alone cannot establish the nature or mechanism of such interactions.

CONCLUSIONS

This study demostrated that rice bran powder and eggshell powder function as a synergistic system that supports fungal growth and facilitates calcium carbonate ($CaCO_3$) biomineralization, resulting in a calcite-rich biomass-mineral product with potential for future evaluation in cementitious systems. The results indicated that rice bran served as an organic nutrient source supporting fungal metabolism and biomass development, as evidenced by substrate mass reduction in the fungal treatments (T2 and T5) and the detection of amorphous biomass through XRD and protein-associated functional groups through FTIR. Simultaneously, eggshell powder served as a calcium source and contributed to pH buffering, with T5 reaching pH 8.14 by Day 28, a condition associated with calcite precipitation. Comprehensive characterization of T5 revealed the coexistence of organic and inorganic components. XRD analysis identified amorphous biomass and crystalline calcite, while FTIR spectroscopy identified organic functional groups and carbonate-associated vibrational bands. Furthermore, XRF analysis showed the presence of calcium, silica, and potassium, complementing the XRD and FTIR evidence of the mineral and organic components. These findings provided a basis for further investigation of calcite-rich products derived from rice bran and chicken eggshells. Under the conditions investigated, rice bran and eggshell powder served as alternative organic nutrient and calcium sources, respectively, for fungal-mediated biomineralization. By utilizing rice bran and eggshell powder, the system reduces the need for expensive or corrosive external chemical inputs and offers a sustainable alternative to conventional chemical nutrient and calcium sources for producing calcite-rich biocomposites.

Acknowledgements

This work was financially supported by Ardhi University (ARU) research project TZ2021IUC042A104 VLIRUOS Institutional University Cooperation (IUC) Programme at Ardhi University (ARU), Tanzania, Sub-project 2.

REFERENCES

1. Adetunji, M. A., Oyeleye, O. I., Oluremi, A. (2018). Assessment of building collapse in Lagos Island, Nigeria. *American Journal of Sustainable Cities and Society*, *1*(7). https://doi.org/10.26808/rs.aj.i7v1.04
2. Ahmed, S., Mustafa, G., Arshad, M., Rajoka, M. I. (2017). Fungal biomass protein production from *Trichoderma harzianum* using rice polishing. *BioMed Research International*, 1–9. https://doi.org/10.1155/2017/6232793
3. Bindschedler, S., Cailleau, G., Verrecchia, E. (2016). Role of fungi in the biomineralization of calcite. *Minerals*, *6*(2), 41. https://doi.org/10.3390/min6020041
4. Cahya, M., Marfuah, N. (2014). Identification of Calcium Carbonate ($CaCO_3$) Characteristics from Different Kinds of Poultry Eggshells Using X-Ray Diffraction (XRD) and Fourier Transformation Infra-Red (FTIR): *2014 International Conference on Physics and its Applications (ICOPIA-14)*. https://doi.org/10.2991/icopia-14.2015.27
5. Denardi, T., Leal, C. A., Massarolo, K. C., Badiale-Fulong, E. (2019). Profile of phenolic compounds released from rice bran by *Rhizopus oryzae* and *Trichoderma reesei*: Their relation with hydrolases activity. *Journal of Food Science*, *84*(6), 1382–1389. https://doi.org/10.1111/1750-3841.14646
6. Jaf, D. K., Abdulrahman, P. I. (2023). A review on self-healing concrete. *Advanced Materials Research*, *1175*, 139–148. https://doi.org/10.4028/p-52lej6
7. Kioko, J. M. (2014). Causes of building failures in Africa: A case study on collapsing structures in Kenya. *IOSR Journal of Mechanical and Civil Engineering*, *11*(3), 9–10. https://doi.org/10.9790/1684-11370910
8. Le, N. H., Thu, T. T. T., Tan Dung, N. (2026). Applying

eggshell powder to improve the soil quality of durian orchard gardens in Dong Thap Province. *VNU Journal of Science: Earth and Environmental Sciences*. https://doi.org/10.25073/2588-1094/vnuees.5485

9. Lee, D., Lee, S., Jang, E., Shin, H., Moon, B., Lee, C. (2016). Metabolomic profiles of *Aspergillus oryzae* and *Bacillus amyloliquefaciens* during rice koji fermentation. *Molecules*, *21*(6), 773. https://doi.org/10.3390/molecules21060773
10. Lelamurnik, D. A. R., Abd Rashid, N. Y., Jamaluddin, A., Sharifudin, S. A., Abd Kahar, A., Long, K. (2017). Cosmeceutical potentials and bioactive compounds of rice bran fermented with single and mix culture of *Aspergillus oryzae* and *Rhizopus oryzae*. *Journal of the Saudi Society of Agricultural Sciences*, *16*(2), 127–134. https://doi.org/10.1016/j.jssas.2015.04.001
11. Li, Q., Csetenyi, L., Gadd, G. M. (2014). Biomineralization of metal carbonates by *Neurospora crassa*. *Environmental Science & Technology*, *48*(24), 14409–14416. https://doi.org/10.1021/es5042546
12. Li, T., Hu, Y., Zhang, B. (2018). Biomineralization induced by *Colletotrichum acutatum*: A Potential strategy for cultural relic bioprotection. *Frontiers in Microbiology*, *9*, 1884. https://doi.org/10.3389/fmicb.2018.01884
13. Lopes, C. D. C. A., Limirio, P. H. J. O., Novais, V. R., Dechichi, P. (2018). Fourier transform infrared spectroscopy (FTIR) application chemical characterization of enamel, dentin and bone. *Applied Spectroscopy Reviews*, *53*(9), 747–769. https://doi.org/10.1080/05704928.2018.1431923
14. Magafu, F. F., Li, W. (2010). Causes of cracks on structures in Ngara-Tanzania. *Engineering*, *2*(12), 958–961. https://doi.org/10.4236/eng.2010.212121
15. Mariyam, M., Sunarintyas, S., Yuliatun, L., Khuzaimah, I., Nuryono, N. (2025). Fabrication of calcite calcium carbonate from eggshells biogenic waste through carbonation method. *Jurnal Kimia Valensi*, *11*(1), 9–17. https://doi.org/10.15408/jkv.v11i1.41914
16. Mony, B. (2015). Effect of chicken egg shell powder solution on early enamel carious lesions: An invitro preliminary study. *Journal of Clinical and Diagnostic Research*. https://doi.org/10.7860/JCDR/2015/11404.5656
17. Niemeyer, J., Chen, Y., Bollag, J. -M. (1992). Characterization of humic acids, composts, and peat by diffuse reflectance Fourier-Transform infrared spectroscopy. *Soil Science Society of America Journal*, *56*(1), 135–140. https://doi.org/10.2136/sssaj1992.03615995005600010021x
18. Ningrum, R. A., Humaidi, S., Sihotang, S., Bonardo, D., Estananto. (2022). Synthesis and material characterization of calcium carbonate ($CaCO_3$) from the waste of chicken eggshells. *Journal of Physics: Conference Series*, *2193*(1), 012009. https://doi.org/10.1088/1742-6596/2193/1/012009
19. Ohenhen, L. O., Shirzaei, M. (2022). Land subsidence hazard and building collapse risk in the coastal city of Lagos, West Africa. *Earth's Future*, *10*(12). https://doi.org/10.1029/2022ef003219
20. Ohshima, Y., Takada, D., Namai, S., Sawai, J., Kikuchi, M., Hotta, M. (2015). Antimicrobial characteristics of heated eggshell powder. *Biocontrol Science*, *20*(4), 239–246. https://doi.org/10.4265/bio.20.239
21. Omoregie, A. I., Muda, K., Bakri, M. K. B., Rahman, M. R., Yusof, F. A. M., Ojuri, O. O. (2024). Calcium carbonate bioprecipitation mediated by ureolytic bacteria grown in pelletized organic manure medium. *Biomass Conversion and Biorefinery*, *14*(12), 13005–13026. https://doi.org/10.1007/s13399-022-03239-w
22. Parikh, S. J., Chorover, J. (2005). FTIR spectroscopic study of biogenic Mn-oxide formation by *Pseudomonas putida* GB-1. *Geomicrobiology Journal*, *22*(5), 207–218. https://doi.org/10.1080/01490450590947724
23. Preston, L. J., Shuster, J., Fernández-Remolar, D., Banerjee, N. R., Osinski, G. R., Southam, G. (2011). The preservation and degradation of filamentous bacteria and biomolecules within iron oxide deposits at Rio Tinto, Spain. *Geobiology*, *9*(3), 233–249. https://doi.org/10.1111/j.1472-4669.2011.00275.x
24. Priya, N. J., Kannan, M. (2025). *In Vitro* biomineralization of calcite by *Bacillus velezensis* SR2307 and *Pseudomonas aeruginosa* JNP 01 and its characterization studies. *Geomicrobiology Journal*, *42*(7), 567–575. https://doi.org/10.1080/01490451.2025.2487086
25. Saxena, A., Sang, Abraham, A. (2024). Bio-concrete for the modern era: Paving the way for future construction. *Journal of Ceramic Processing Research*, *25*(6), 1122–1141. https://doi.org/10.36410/JCPR.2024.25.6.1122
26. Setiyawan, A. I., Pratiwi, D., Karimy, M. F., Fauziah, S. (2021). Minerals composition and characterization of the hatchery eggshell waste treated with different preparation methods. *Jurnal Ilmu Dan Teknologi Hasil Ternak*, *16*(3), 144–152. https://doi.org/10.21776/ub.jitek.2021.016.03.1
27. Simpen, I. N., Winaya, I. N. S., Suarsana, I. K., Sugita, I. K. G. (2024). Green nanocomposite of silica-supported CaO: Synthesis by sol-gel method and characterization: -. *EUREKA: Physics and Engineering*, (6), 151–161. https://doi.org/10.21303/2461-4262.2024.003407
28. Singh, H., Bhandari, M. (2024). A contemporary review on progressive collapse. *IOP Conference Series: Earth and Environmental Science*, *1326*(1), 012027. https://doi.org/10.1088/1755-1315/1326/1/012027

29. Smidt, E., Lechner, P., Schwanninger, M., Haberhauer, G., Gerzabek, M. H. (2002). Characterization of waste organic matter by FT-IR spectroscopy: Application in waste science. *Applied Spectroscopy*, *56*(9), 1170–1175. https://doi.org/10.1366/000370202760295412
30. Sompech, S., Dasri, T., Thaomola, S. (2016). Preparation and characterization of *Amorphous Silica* and calcium oxide from agricultural wastes. *Oriental Journal of Chemistry*, *32*(4), 1923–1928. https://doi.org/10.13005/ojc/320418
31. Spelta, J. S. D. O., Galdino, A. G. D. S. (2018). Bioceramic composite: Hen's eggshell characterization and main applications. *Revista Ifes Ciência*, *4*(1), 9–20. https://doi.org/10.36524/ric.v4i1.323
32. Taoufik, J., Issam, A., Mohammed, R. (2024). Investigations into cracks causes in educational building: A case study. *Civil Engineering and Architecture*, *12*(3), 1841–1853. https://doi.org/10.13189/cea.2024.120342
33. Udhaya, S., Vandhana Devi, V., Philips, J., Lija, R. L. (2023). Experimental study on bio-concrete for sustainable construction. *Materials Today: Proceedings*. https://doi.org/10.1016/j.matpr.2023.03.676
34. Vasquez, F. Y. C., Fuentes, A. G. P., Casinillo, L. F. (2024). Evaluating eco-friendly soil neutralizers: The use of pulverized eggshells and clam shells in enhancing rice field soil acidity. *EDUCATUM Journal of Science, Mathematics and Technology*, *11*(1), 101–109. https://doi.org/10.37134/ejsmt.vol11.1.10.2024
35. Wainaina, S., Kisworini, A. D., Fanani, M., Wikandari, R., Millati, R., Niklasson, C., Taherzadeh, M. J. (2020). Utilization of food waste-derived volatile fatty acids for production of edible *Rhizopus oligosporus* fungal biomass. *Bioresource Technology*, *310*, 123444. https://doi.org/10.1016/j.biortech.2020.123444
36. Wikandari, R., Nisrina, H., Setiowati, A. D., Millati, R. (2025). Enhanced bioaccumulation of essential minerals in filamentous fungal biomass during cultivation to produce high quality vegan food. *Polish Journal of Food and Nutrition Sciences*, 274–282. https://doi.org/10.31883/pjfns/209007
37. Yan, Z., Nakashima, K., Takano, C., Kawasaki, S. (2024). Feasibility study of enhancing enzyme-induced carbonate precipitation with eggshell waste for sand solidification. *Biogeotechnics*, *2*(4), 100108. https://doi.org/10.1016/j.bgtech.2024.100108
38. Yusuf, M. O. (2023). Bond characterization in cementitious material binders using Fourier-transform infrared spectroscopy. *Applied Sciences*, *13*(5), 3353. https://doi.org/10.3390/app13053353
39. Zhang, Y. S., Liu, Y., Sun, X. D., Zeng, W., Xing, H. P., Lin, J. Z., Kang, S. B., Yu, L. (2024). Application of microbially induced calcium carbonate precipitation (MICP) technique in concrete crack repair: A review. *Construction and Building Materials*, *411*, 134313. https://doi.org/10.1016/j.conbuildmat.2023.134313
40. Zhao, H., Zhao, Y., Tong, Y. (2025). Crack repair in existing concrete structures: Progress in research and applications. *Journal of Asian Concrete Federation*, *11*(1). https://doi.org/10.18702/acf.2024.11.1.15